

Inhibition of Copper Corrosion by Two Calixarenic Molecules in 0.5M H₂SO₄ Solutions: Electrochemical and Surface Studies

Naziha M'hanni ¹, Mouhsine Galai ^{1,*} , Moussa Ouakki ^{2,3}, Mohamed Ebn Touhami ¹, El Housseine Rifi ¹, Zouhair Asfari ⁴

¹ Advanced Materials and Process Engineering, Faculty of Sciences, Ibn Tofail University, PO Box 133, 14000, Kenitra, Morocco

² Laboratory Organic Synthesis and Extraction Processes, Faculty of Science, University Ibn Tofail, BP 133, 14000 Kenitra, Morocco

³ National Higher School of Chemistry (NHSC), University Ibn Tofail BP, Kenitra, 133-14000, Morocco

⁴ Laboratory of Molecular Engineering Applied to the Analysis, IPHC, UMR 7178 CNRS, University of Strasbourg, ECPM, 25 street Becquerel, 67087 Strasbourg Cedex 2, France

* Correspondence: galaimouhsine@gmail.com (M.G.);

Scopus Author ID 55867997200

Received: 18.06.2022; Accepted: 30.07.2022; Published: 22.11.2022

Abstract: Comparative study of the inhibition and adsorption properties of two Calixarenic organic molecules type 2,2' - ((15,35,55,75 – tetra – tert – butyl - 32,72 – dihydroxy - 1,3,5,7 (1,3) tetrabenzenacyclooctaphane-12,52-diyl) bis(oxy))diacetic acid and 5-(4-(tert-butyl)-2-(5-(tert-butyl)-2-hydroxy-3-methylbenzyl)-6-methylphenoxy)pentanoic acid named TTB and TB2HMHA, as good corrosion inhibitors in the 0.5M sulfuric medium utilizing potentiodynamic polarization (PDP), electrochemical impedance spectroscopy (EIS), and procedures for scanning electron microscopy (SEM). The experimental outcomes revealed that the TTB and TB2HMHA effectively against copper corrosion in 0.5 M H₂SO₄. This work's novelty is using two green syntheses of new heterocyclic compounds (TTB and TB2HMHA) as ecological inhibitors of acid corrosion of m-steel. As a result, the inhibitory efficiency has been reached at an optimum value of 97.9% for TTB. EIS data demonstrated that the copper corrosion reaction happens mainly via diffusion control and that the organic species' corrosion rates and inhibition effectiveness were computed. The inhibition mechanisms are predicted from the evolution of the inhibition effectiveness versus inhibitor concentration and temperature. The achieved findings suggested that molecular and protonated organic species of the two Calixarenes contributed to the observed inhibitory action. Furthermore, SEM analysis confirmed the high inhibitory effect of these two products by adsorption on the copper surface. In addition, the rise in temperature did not significantly affect the inhibitory efficiency values, which confirmed the high resistance of the composite.

Keywords: electrochemical impedance spectroscopy; calixarene; corrosion of copper; H₂SO₄; potentiodynamic polarization.

© 2022 by the authors. This article is an open-access article distributed under the terms and conditions of the Creative Commons Attribution (CC BY) license (<https://creativecommons.org/licenses/by/4.0/>).

1. Introduction

Various industrial electronics and communications applications utilize copper as a conductor for electrical lines, pipelines, and Services involving industrial water, including seawater, heat exchangers, heat conductors, etc. Thus, copper is one of the more important metals because of its outstanding thermal and electrical conductivity, suitability for mechanical processing, and relatively noble properties.

This type of metal is commonly applied in cooling and heating applications and is utilized in various applications. The reduction in the effectiveness of the heating system is affected most frequently by scaling and corrosion products that harm the transfer of heat. Therefore, it is necessary to clean them regularly using acidic solutions such as sulfuric acid (H₂SO₄). Corrosion inhibitors effectively eliminate the undesirable destructive effect and prevent metal dissolution. Unfortunately, the majority of inhibitors commercially available are toxic components that need to be substituted with new eco-friendly inhibitors[1].

The application of corrosion inhibitors for copper in such conditions is required since a passive protective film can not be expected. The ability to inhibit the corrosion of copper in various aqueous environments has interested numerous researchers utilizing many inhibitors. These investigations show that many organic and inorganic compounds can prevent copper from corrosion [2-6]. The availability of heteroatoms, including nitrogen (N), sulfur (S), and phosphorous (P) in the inhibitor molecule enhanced its ability to prevent rusting. Among these organic molecules and their derivatives, there are azoles [7,8], amino acids [9], and many others, there are very toxic compounds.

Generally, the nature and charge of the metal surface, the adsorption mechanism, the chemical structure, and the inhibitor's ability to adsorb on a metal surface depend on the kind of electrolyte medium used. [10]. However, applying inorganic or organic products and their derivatives effectively protects copper and its alloys in an aggressive medium [11, 12].

This is ascribed to the chelation effect of the heterocyclic element of the chemical compound and the formation of a protective barrier film between the metal surface and the chemical compound, preventing the dissolution of the metal from the corrosion process. The protective layer is assigned to the availability of either emptied orbitals in the copper atom that form coordinative bonds with atoms that donate electrons, including nitrogen (N), sulfur (S), phosphorous (P), or the aromatic rings through the nitrogen-containing heterocyclic part of the inhibitor [13].

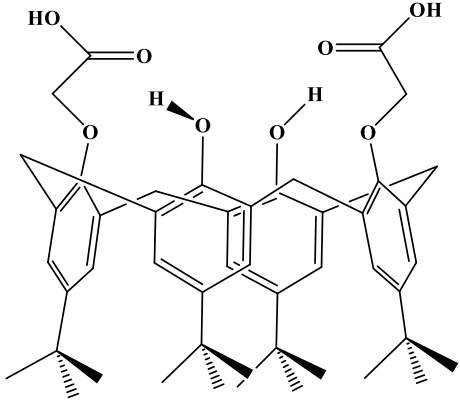
Organic compounds are usually employed to prevent the corrosion of metals as inhibitors in acidic solutions [14-32]. However, the inhibition effect of organic species has been found to be dependent on [33,34]: (i) the chemical structure of the inhibitor, (ii) the charge of the metal surface, and (iii) the nature of contacts between the inhibitor species and the surface of the metal.

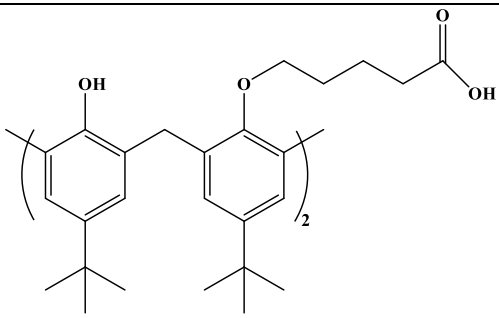
The challenge of this work is the green synthesis of new heterocyclic compounds (TTB and TB2HMHA) as ecological inhibitors of acid corrosion of m-steel. The inhibitory action of organic compounds was evaluated through several techniques already described in the literature (EIS and PDP). SEM/EDS has located the steel that was buried and Contact angle measurements (θ). Experimental data have shown that additives TTB and TB2HMHA are effective against the

The electrochemical Tests were conducted utilizing a three-electrode cell consisting of a reference electrode (Ag/AgCl), a counter electrode (platinum), and a working electrode (copper). The composition (by weight %) of copper utilized for the electrochemical experiments is: P(0.019 %), Pb(0.015 %), Sn(0.009 %), Ni(0.003%), Sb(<0.002%), Ag(<0.005%), C(<0.005 %), Fe(<0.001 %), As(<0.001 %), Mn(<0.001 %), Al(<0.001 %), Bi(<0.001 %), S(<0.001 %) and the rest is Cu".

The aggressive solution utilized in the present investigation was a sulfuric acid (0.5M H₂SO₄) prepared by diluting a commercially concentrated acid of 98% with distilled water.

In addition, the EIS tests were performed at open circuit potential (OCP)utilizing a transfer function analyzer in the100 kHz-10 mHz frequency range of 10 points per decade. The applied AC signal's amplitude was 10 mV. The EIS data were executed using a Volta Lab PGZ 100 model potentiostat controlled by a PC and Voltalab 4.0 analysis software. The measured impedance data were analyzed using the Zview software package and fitted in terms of an appropriate equivalent electric circuit. The molecular structure of the investigated inhibitors is displayed in Table 1.

Abbreviation	Chemical structure	IUPAC Name/ molecular formula/molar mass
TTB		2,2'-((15,35,55,75-tetra-tert-butyl-32,72-dihydroxy-1,3,5,7(1,3)-tetrabenzenacyclooctaphane-12,52-diyl)bis(oxy))diacetic acid $C_{48}H_{60}O_8$ 765 g/mol

Abbreviation	Chemical structure	IUPAC Name/ molecular formula/molar mass
TB ₂ HMHA		5-(4-(tert-butyl)-2-(5-(tert-butyl)-2-hydroxy-3-methylbenzyl)-6-methylphenoxy)pentanoic acid
		C ₅₁ H ₇₀ O ₆
		778 mol

3. Results and Discussion

3.1. Stationary electrochemical study.

Figure 1 presents the anodic and cathodic polarization curves for copper in 0.5 M H₂SO₄ medium in the absence and the presence of TTB and TB₂HMHA at different concentrations and 298K.

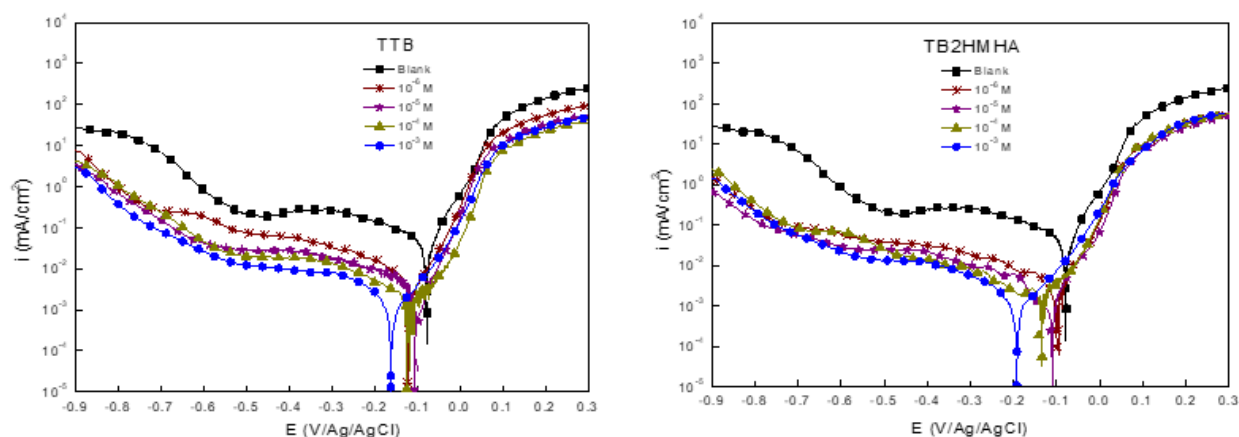


Figure 1. Representation of the copper in 0.5 M H₂SO₄ medium anodic and cathodic polarization curves in the without and the existence of TTB and TB₂HMHA at different concentrations and 298K.

An initial analysis of these curves shows that addition has an impact on both the anodic and cathodic reactions of the TTB and TB₂HMHA compounds. The addition of the inhibitor in 0.5 M H₂SO₄ solution significantly retarded both cathodic (hydrogen evolution) and anodic reactions (stainless dissolution). This behavior reflects the inhibitory action of both products [36]. In addition, the polarization plots were displaced to lower corrosion current densities (*i*_{corr}) and smaller negative corrosion potentials (*E*_{corr}) after adding both examined molecules. This shift in PDP plots was more marked in the cathodic curves, which corresponds to the dominant cathodic inhibition mechanism of the calixarenes molecules. However, the corrosion potential showed a significant change in the presence of the calixarenes. Therefore, the two compounds can be classified as cathodic-type inhibitors [37]. According to Figure 1, the anodic branches followed typical Tafel behavior throughout a wide range of current and potential. It implies that reliable determination of anodic slopes is possible. However, on the cathodic branches of the curves, there was no evidence of a linear Tafel zone. The values of the anodic Tafel slopes (β_a). The

measurements of the electrochemical parameters derived from the collected polarization curves are shown in Table 2: corrosion current density (i_{corr}), corrosion potential (E_{corr}), cathodic Tafel slopes, and potential corrosion coefficient (E_{corr}), as well as the corrosion inhibitor efficiency $\eta_{\text{PP}}(\%)$.

Table 2. Inhibition efficiency and electrochemical parameters were determined from the copper polarization curves in 0.5 M H_2SO_4 with and without TTB and TB2HMHA.

Medium	Conc. (mol /L)	$-E_{\text{corr}}$ (mV/Ag/AgCl)	i_{corr} ($\mu\text{A cm}^{-2}$)	Tafel slopes (mV/dec)		η_{PP} %
				$-\beta_c$	β_a	
0.5 M H_2SO_4	--	79 ± 1.5	29.0 ± 1.7	204 ± 2.5	59.0 ± 1.2	--
TTB	10^{-3}	155 ± 2.3	0.6 ± 0.05	184 ± 2.8	56.0 ± 1.8	97,9
	10^{-4}	125 ± 1.8	1.6 ± 0.09	188 ± 3.1	57.5 ± 1.6	94,4
	10^{-5}	98 ± 1.0	2.0 ± 0.1	196 ± 2.6	58.3 ± 2.0	93,1
	10^{-6}	121 ± 2.1	2.2 ± 0.1	191 ± 1.9	60.2 ± 1.7	92,4
TB2HMHA	10^{-3}	189 ± 2.4	0.7 ± 0.06	179 ± 2.4	65.2 ± 2.1	97,5
	10^{-4}	128 ± 1.6	1.0 ± 0.08	176 ± 2.3	57.2 ± 2.0	96,5
	10^{-5}	101 ± 1.4	1.4 ± 0.04	165 ± 1.8	62.7 ± 1.8	95,2
	10^{-6}	96 ± 1.3	1.5 ± 0.09	191 ± 2.5	61.9 ± 1.9	94,8

The analysis in Table 2 demonstrates a significant diminution in the i_{corr} values with increasing concentration of the examined compounds, which implies an enhancement in the effectiveness of inhibitors. After adding the two calixarene derivatives, the E_{corr} shifts to more cathodic values. The literature reported that if the absolute shift in E_{corr} is greater than 85 mV, compared to the E_{corr} for the blank medium, the inhibitor can be considered an anodic or cathodic type inhibitor. However, they can be classified as mixed-type inhibitors if this shift is smaller than 85 mV [38]. In the present investigation, less than 85 mV was the highest shift of the E_{corr} readings, indicating that TTB and TB2HMHA act as cathodic-type inhibitors.

The two additives studied, TTB and TB2HMHA, are, therefore, classified as the best with a maximum inhibition efficiency of 97.9% for a concentration of 10^{-3}M , in agreement with the lowest corrosion current density value of $0.6 \mu\text{A}/\text{cm}^2$. This excellent efficiency is explained by the presence of high electronic densities on the molecules due to the existence of non-binding doublets of heteroatoms (N and O) and electrons (π) of aromaticity, which promotes the process of adsorption on metal [39-42]. However, this stationary electrochemical technique remains very limited in characterizing complex mechanisms involving several reactive stages and having different characteristic kinetics. Thus, the use of transient techniques becomes essential.

3.2. Electrochemical impedance spectroscopy.

The effect of changing the concentrations of the two studied products on the impedance behavior of copper in 0.5 M H_2SO_4 are displayed in Figure 2, and Bode planes in Figure 3. The curves show a similar type of Nyquist plot for copper in the existence of different concentrations of Calixarene (TTB and TB2HMHA). The equivalent electrical circuit (Randle equivalent circuit) utilized to simulate the impedance diagrams has been presented in Figure 4, where R_s denotes the resistance of solution, represents the charge transfer resistance and Q_{ct} is the constant phase element of the double layer. The presence of one single semi-circle revealed a pure charge transfer process during dissolution. The diameter of the semi-circle enhanced with the inhibitor concentration, indicating that the formed inhibitive film was reinforced by the addition of TTB

and TB2HMHA[43-48]. The deviations from the perfect circular form, i.e., depression, are often linked to the frequency dispersion of interfacial impedance[49,50].

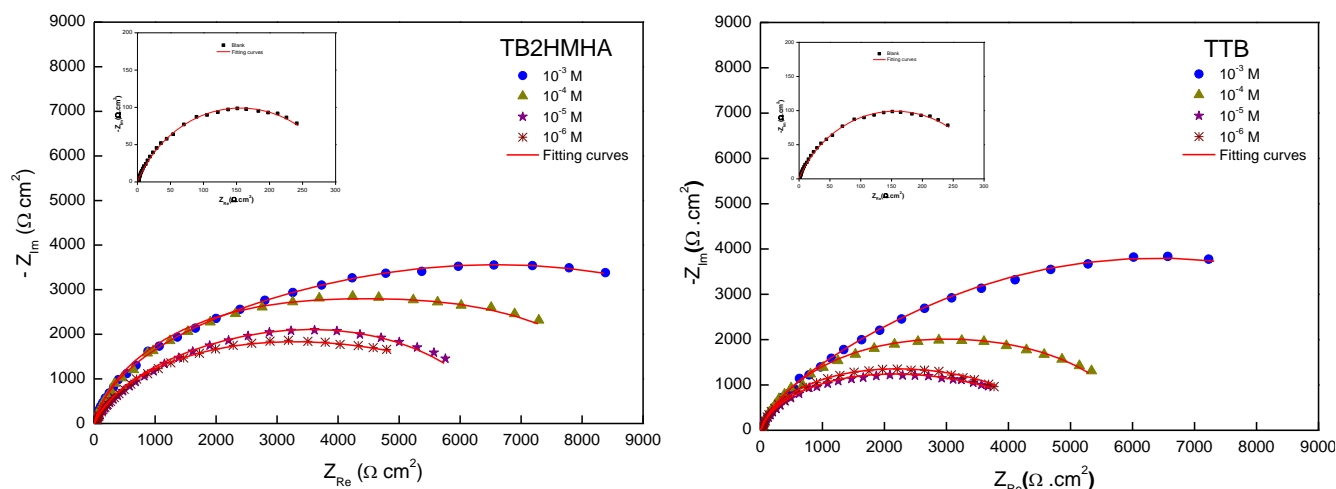


Figure 2. Nyquist plots of copper in 0.5 M H₂SO₄, both with and without various amounts of TTB and TB2HMHA.

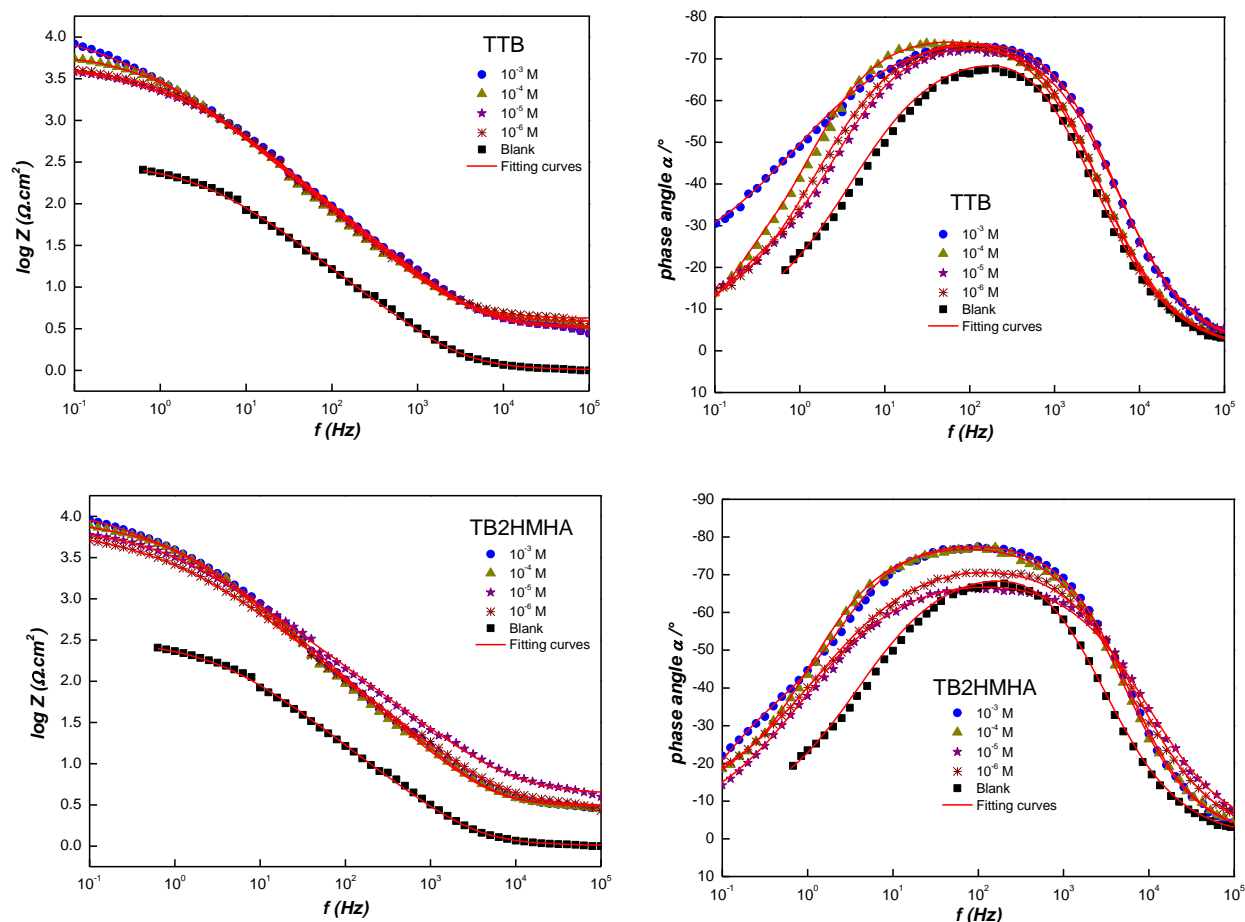


Figure 3. Bode spectrum of copper in 0.5 M H₂SO₄ solution in the absence and the presence of TTB and TB2HMHA at different concentrations.

But in solution, the inhibitory efficiency of 0.5 M H₂SO₄ decreased when the additive concentration decreased and reached a high efficiency of 97.9% for TTB and 97.3%

for TB2HMHA at 10⁻³M concentration of additives. On the other hand, the decrease of Cdl values that increase as the inhibitor concentration increases is probably due to the diminution of the local dielectric constant and/or the increase of the electric double-layer thickness. This indicates that TTB and TB2HMHA adsorb on the copper/acid interface[51,52].

The Bode spectrum obtained for copper in the absence and the presence of TTB and TB2HMHA (Figure 3) shows two maximum phases at intermediate and low frequencies. The Bode Representation confirms using two electrical circuits to simulate experimental data.

Table 3. Electrochemical characteristics and associated inhibition effectiveness for corrosion of the copper in 0.5 M H₂SO₄ whether various concentrations are present or absent of TTB and TB2HMHA at 298 K.

Inhibitors	C (M)	R _s (Ω.cm ²)	Q _r (μFcm ²)	n _r	R _r (Ω.cm ²)	Q _{ct} (μF cm ²)	n _{ct}	R _{ct} (Ω cm ²)	R _p (Ω cm ²)	θ	η _{imp} %
Blank	--	0.7±0.2	-	-	-	475±3.5	0.720±0.01	350±2.5	350	--	--
TTB	10 ⁻³	3.2±1.0	43.1±1.8	0.848±0.007	12239±3.4	50.5±1.2	0.686±0.008	4703±4.8	16942	0.979	97,9
	10 ⁻⁴	3.7±1.2	49.5±2.3	0.824±0.01	4878±2.5	486.7±3.4	0.850±0.009	1229±2.6	6107	0.942	94,2
	10 ⁻⁵	2.7±0.9	52.6±2.5	0.786±0.009	2951±1.8	495.5±3.8	0.645±0.01	1848±2.4	4799	0.927	92,7
	10 ⁻⁶	2.5±0.8	41.1±1.7	0.852±0.008	2516±2.3	293.4±2.9	0.631±0.007	2208±3.2	4724	0.926	92,6
TB2HMHA	10 ⁻³	4.7±1.3	25.4±1.0	0.900±0.01	3846±3.7	105.3±1.5	0.610±0.01	9287±5.2	13133	0.973	97,3
	10 ⁻⁴	3.0±1.2	34.1±1.3	0.880±0.008	5941±4.0	285.8±2.4	0.841±0.009	3101±1.8	9042	0.961	96,1
	10 ⁻⁵	4.2±1.5	43.4±2.0	0.780±0.009	4846±2.8	147.7±1.3	0.779±0.01	2343±2.6	7189	0.951	95,1
	10 ⁻⁶	3.0±1.2	45.2±2.3	0.826±0.007	2258±2.6	170.5±1.4	0.635±0.008	4678±4.1	6936	0.949	94,9

The data in Table 3 shows that as the inhibitor concentrations increase, the R_p values increase, but the Cdl values tend to decrease. These observations reflect a noticeable increase in the thickness of the film formed and a decrease in its permeability [53]. Consequently, the decrease in Q_f values shows that the adsorption layer formed by these compounds on the metal surface is stable [54]. The reduction in Q_f values could occur due to a local decrease in increasing the thickness of the double layer or/and the dielectric constant. It has been related to the replacement of H₂O molecules by the adsorption of organic species on the steel surface[55-57].

Based on the Helmholtz model, the capacity of the double layer (Cdl) can be determined utilizing the equation (1)[58,59]

$$C_{dl} = \frac{\epsilon_0 \epsilon S}{e} \quad (1)$$

where, e represents the deposit thickness, ε₀ is the Permittivity of the solution (8.854×10⁻¹⁴ F cm⁻¹), ε stands for the dielectric constant, and S is the surface of the steel.

The inhibition effectiveness (E%) improves as the inhibitor concentrations increase. This is related to an increase in R_p values, which shows better adsorption of the investigated molecules of inhibitors on the steel's surface. These findings have been explained and confirmed by many authors [60,61]. The electrical equivalent circuit modeling from EIS data is displayed in Figure 4.

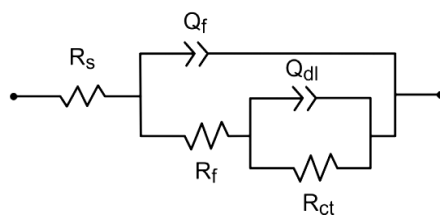


Figure 4. Equivalent circuit for the electrochemical impedance spectra.

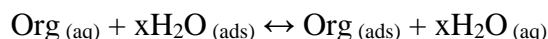
As stated previously, it was a two-time constant model because of the existence of both passive and corrosive regions on such surfaces. The passive regions are related to the oxide film over the surface of the copper, while the corrosive regions are referred to the breakdown of the oxide film. In this investigation, R_s represents the resistance of solution (electrolyte), R_f and R_{ct} are related to the surface film resistance and the charge transfer resistance linked to the corrosion process taking place on the surface of copper. Q_f and Q_{dl} are the surface film capacitance and the double layer capacitance, respectively. The EIS diagrams were fitted, and the determined electrochemical parameters using the equivalent circuit model (Figure 4) are presented in Table 3. CPE was used as the substitute for the capacitor to fit more exactly EIS diagrams. The CPE impedance can be described by equation 2 [62,63].

$$Z_{CPE} = \frac{1}{Y(j\omega)n_{dl}} \quad (2)$$

where, Y represents the CPE magnitude, ω is the angular frequency, and n stands for an empirical exponent that provides the deviation from the ideal capacitive behavior [64, 65]. According to the n values, CPE can represent resistance ($n = 0$), capacitance ($n = 1$), inductance ($n = -1$), and Warburg impedance ($n = 0.5$) [66-68].

3.3. Adsorption isotherm.

An adsorption investigation has been carried out to elucidate the inhibition effect of organic molecules on copper corrosion. This effect occurs through two major types of adsorption: chemical and physical adsorption. In an aqueous solution, the adsorption process of these inhibitors is generally coupled with the desorption of water molecules that are pre-adsorbed on the copper surface. This adsorption is therefore regarded as a phenomenon of substitutional adsorption, as illustrated by the following reaction:



where, x denotes the number of water molecules substituted by the inhibitor molecule. Several adsorption isotherms are used to evaluate the adsorption process on the copper surface (Langmuir isotherm, Temkin, Frumkin, etc.) [37]. The obtained EIS values are investigated for fitting various adsorption isotherms models. Langmuir isotherm displays a good fit to the experimental data within these adsorption models. The Langmuir isotherm is linked to the surface coverage (θ) and the concentration of the organic species (C_{inh}) according to the equation (3) [69]:

$$\frac{C_{inh}}{\theta} = \frac{1}{K_{ads}} + C_{inh} \quad (3)$$

where, K_{ads} represents the adsorption/desorption equilibrium constant. The evolution of the C_{inh}/θ versus C_{inh} of the organic inhibitor is a straight line (Figure 5).

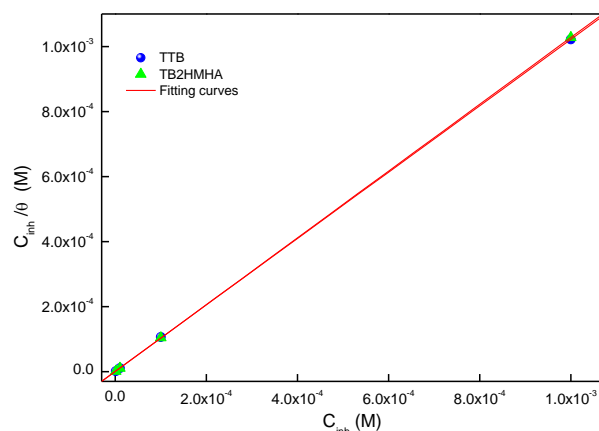


Figure 5. The adsorption isotherm of Langmuir for TTB and TB2HMHA on the copper surface at 298 K.

The Langmuir adsorption isotherm provided a more precise explanation of the adsorption behavior of the species under investigation (Figure 5) [70] because the average values of the linear regression coefficient (R^2) achieved for TTB and TB2HMHA and the slope are very close to 1. The K_{ads} value was shown to be important, that is, 66.2×10^4 (L/mol) of TTB and 197.9×10^4 (L/mol) of TB2HMHA (Table 4), which signifies the greater adsorption; this can be related to the existence of various donor centers, including O, N, and Cl in the functional groups. The free adsorption energy (ΔG_{ads}) was computed utilizing the equation (4):

$$K_{ads} = \frac{1}{55.55} e^{-\frac{\Delta G_{ads}}{RT}} \quad (4)$$

where, R denotes the global gas constant, and T denotes the absolute temperature. The molar concentration of water is given by 55.55 [71].

Table 4. Thermodynamic parameters for adsorption of the inhibitors on copper at 298K.

Inhibitors	K_{ads} (L/mol)	ΔG_{ads} (kJ/mol)	R^2	Slopes
TTB	66.2×10^4	-43.1	0.99999	1.02
TB2HMHA	197.9×10^4	-45.8	1	1.03

Generally, The phrase "physisorption," which refers to the electrostatic interaction between charged inhibitor molecules and the charged surface of the metal, is supported by the values of ΔG_{ads} around or less than -20 kJ/mol [72]; the transfer or charge sharing of electrons from the inhibitor is associated with values around or greater than -40 kJ/mol species to the copper surface to establish a coordinated type of metal, i.e., chemisorption [73]. After the addition of calixarenes molecules, ΔG_{ads} was determined to be -43.1 kJ/mol of TTB and -45.8 kJ/mol of TB2HMHA, indicating the chemical adsorption on the copper surface.

3.4. Effect of temperature.

3.4.1. Potentiodynamicpolarization.

Temperature provides critical input into inhibitor action. It can affect the metal-inhibitor interaction in the corrosive environment and influences the adsorption mode of the inhibitor. It is thus essential to explore the influence of these parameters on the action of calixarene molecules, which is an excellent inhibitor at 298K. In this study, the inhibition efficiency of TTB and TB2HMHA on corrosion of copper in 0.5 M H_2SO_4 alone and after adding the investigated molecules at the optimum concentration ($10^{-3}M$) was performed for temperatures ranging from 298K to 328K. The potentiodynamic polarization plots are presented in Figure 6 and the electrochemical parameters derived from these curves are grouped in Table 5.

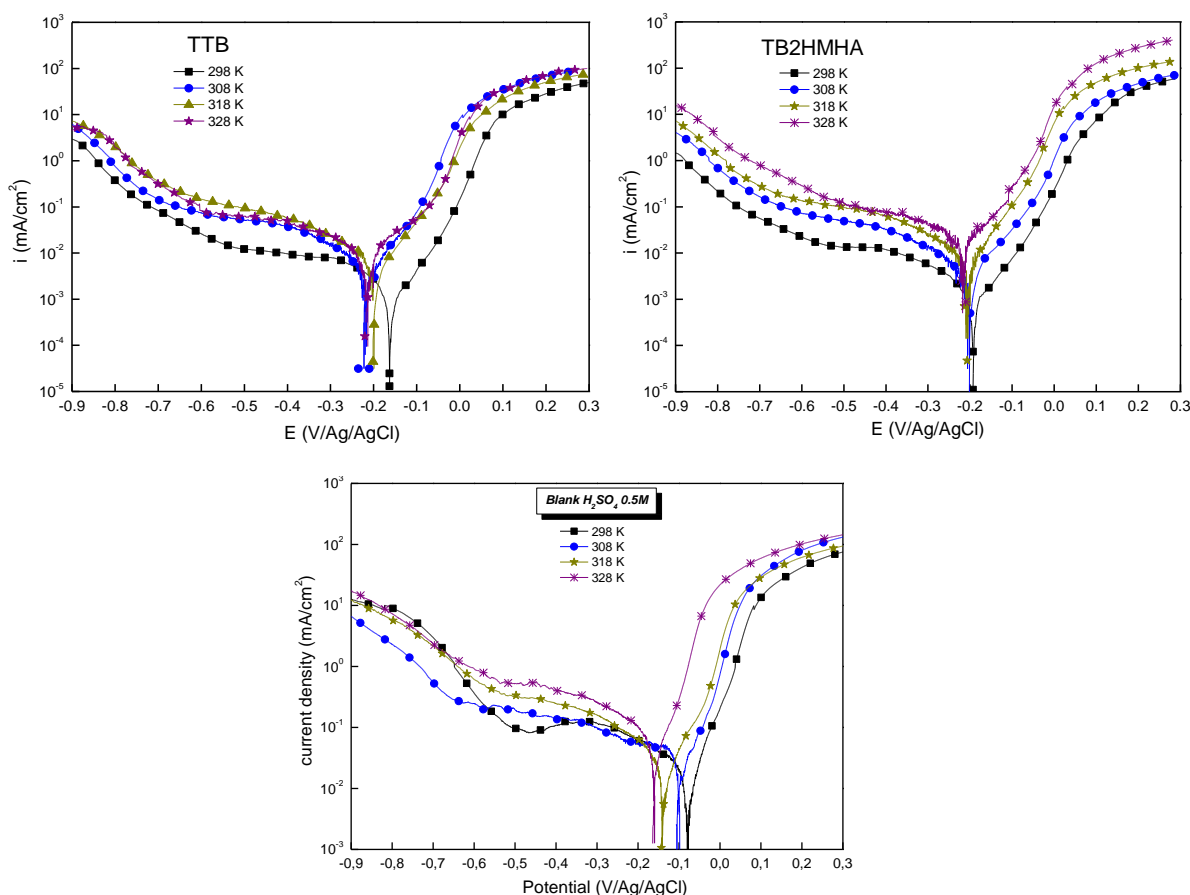


Figure 6. Polarization curves of copper in 0.5 M H_2SO_4 in the absence and the presence of inhibitors at different temperatures.

It can be seen from the Tafel curves that the anodic and cathodic branches increase with temperature. The plots of the cathodic region are parallel, which reflects that the reduction of H^+ -ions on the copper surface is made according to the same pure activation mechanism in all temperature ranges. The data in Table 5 demonstrate that the current densities rise with temperature, thereby leading to a decline in the inhibition effectiveness for both inhibitors at a concentration of $10^{-3}M$ in the H_2SO_4 0.5M medium. Furthermore, it can be remarked that the

inhibition efficacy diminishes slightly after the addition of TTB and TB2HMHA. Thus, these compounds are considered effective inhibitors for copper in sulfuric acid.

Table 5. Electrochemical parameters for copper in 0.5 M H₂SO₄ and the inhibitor 10⁻³M at different temperatures.

Medium	T (K)	-E _{corr} (mV/Ag/AgCl)	i _{corr} (μA cm ⁻²)	Tafel slopes (mV/dec)		η _{PP} %
				-β _c	β _a	
Blank	298	79±1.5	29.0±1.7	204±2.5	59±1.2	--
	308	105±1.6	35.0±1.8	178±2.4	64±1.3	--
	318	142±2.1	56.0±2.0	164±1.9	77±1.8	--
	328	166±2.5	77.0±2.2	182±2.3	52±2.0	--
TTB	298	155±2.3	0,6±0.05	184±2.8	56±1.8	97,9
	308	207±2.4	1,4±0.09	174±1.9	62±1.7	96,0
	318	197±1.9	3,5±0.1	190±2.3	67±2.0	93,7
	328	211±2.6	6,8±0.2	178±2.1	70±2.2	91,1
TB2HMHA	298	189±2.4	0,7±0.06	179±2.4	65,2±2.1	97,5
	308	196±2.8	1,6±0.08	186±1.8	75±2.3	95,4
	318	203±2.6	3,9±0.1	176±2.0	64±1.9	93,0

3.4.2. Thermodynamic parameters for activation.

The variation in the logarithm of the corrosion rate as a function of the inverse of the absolute temperature ($\frac{1000}{T}$) is recorded in Figure 7. The curves obtained in the form of straight lines comply with Arrhenius' law (equation 5).

$$i_{corr} = Ke^{\frac{-E_a}{RT}} \quad (5)$$

where, E_a is the activation energy, R is the perfect gas constant, K is a pre-exponential factor, T is the absolute temperature, and i_{corr} is the corrosion current density.

An alternative formulation of the equation of Arrhenius allows the determination of the values of enthalpy ΔH_a and entropy ΔS_a, according to the following equation (6) [74]:

$$\ln\left(\frac{i_{corr}}{T}\right) = \left[\ln\left(\frac{R}{hN_a}\right) + \left(\frac{\Delta S_a}{R}\right) \right] - \frac{\Delta H_a}{RT} \quad (6)$$

where, h: Planck Constant, N_a: Avogadro number, ΔH_a: Activation Enthalpy, and ΔS_a: Activation Entropy. The variation of $\ln\left(\frac{i_{corr}}{T}\right)$ as a function of the reciprocal of temperature is a line (Figure 7), with a slope equal to $\left(-\frac{\Delta H_a}{RT}\right)$ and an intercept of $\ln\left(\frac{R}{hN_a}\right) + \left(\frac{\Delta S_a}{R}\right)$.

The activation parameters (ΔH_a, ΔS_a, and E_a) calculated from the slopes of the Arrhenius lines in the absence and in the presence of the inhibitors TTB and TB2HMHA are grouped in Table 6.

Table 6. Thermodynamic parameters for corrosion of copper without and with the addition of the inhibitors TTB and TB2HMHA.

0.5 M H ₂ SO ₄			
Compounds	E _a (KJ/mol)	ΔH _a (KJ/mol)	ΔS _a (J/mol.K)
Blank	27.5	24.9	-133.7
TTB	66.7	64.1	-34.0
TB2HMHA	64.8	62.2	-39.1

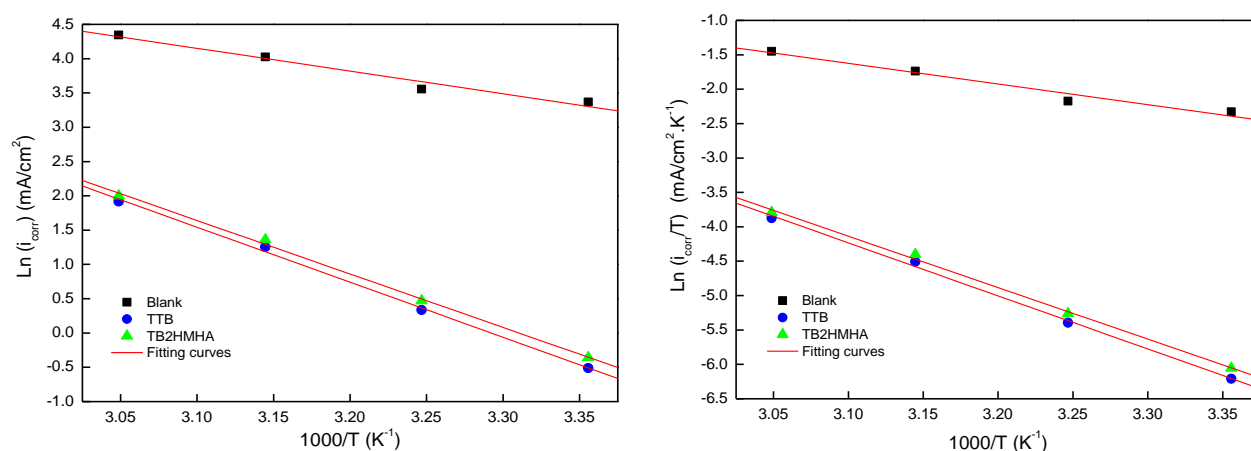


Figure 7. Arrhenius lines for copper in 0.5 M H₂SO₄ medium without and with the addition of the compounds TTB and TB2HMHA 10⁻³M.

From Table 6, it is clear that the E_a values of the solution containing TTB and TB2HMHA are higher than that in the case of the blank medium, confirming the formation of a barrier layer on the copper surface [75]. The higher energy barrier for corrosion after the addition of TTB and TB2HMHA, indicates that the adsorbed inhibitor molecules inhibit the charge/mass exchange interaction that occurs on the surface [76,77]. Therefore, the metal is protected from dissolution. The positive signs of the ΔH values show that the nature of the copper dissolution process is endothermic [78,79]. In the meanwhile, the activation entropies (S_a) rise and become negative in the presence of the inhibitors TTB and TB2HMHA, indicating a reduction in disorder during the conversion of the reagents into activated complex [80,81].

3.5. Surface analysis by SEM -EDX.

SEM micrographs of the copper samples immersed in 0.5 M H₂SO₄ for 6h at 298 K before and after the addition of TTB and TB2HMHA are displayed in Figure 8.

It is observed that the surface of the Cu-substrate immersed in sulfuric acid is severely damaged and attacked with the formation of many pits distributed randomly on the surface. This shows clearly that the copper specimen is subjected to generalized corrosion type over the entire surface in the blank solution. Gray areas attributed to the formation of the iron oxide films

In the presence of 10⁻³M of the compounds TTB and TB2HMHA in the 0.5 M H₂SO₄ solution, Figure 8 shows a smoother, more homogeneous, and brighter surface. Comparing the image obtained without an inhibitor, we can conclude that the surface of the copper is almost free of corrosion. This is due to the formation of the adsorbed layers of the inhibitor on the copper surface. These results confirm the ability of products TTB and TB2HMHA to protect copper and delay its corrosion in H₂SO₄ solutions by limiting electrolyte access to the surface.

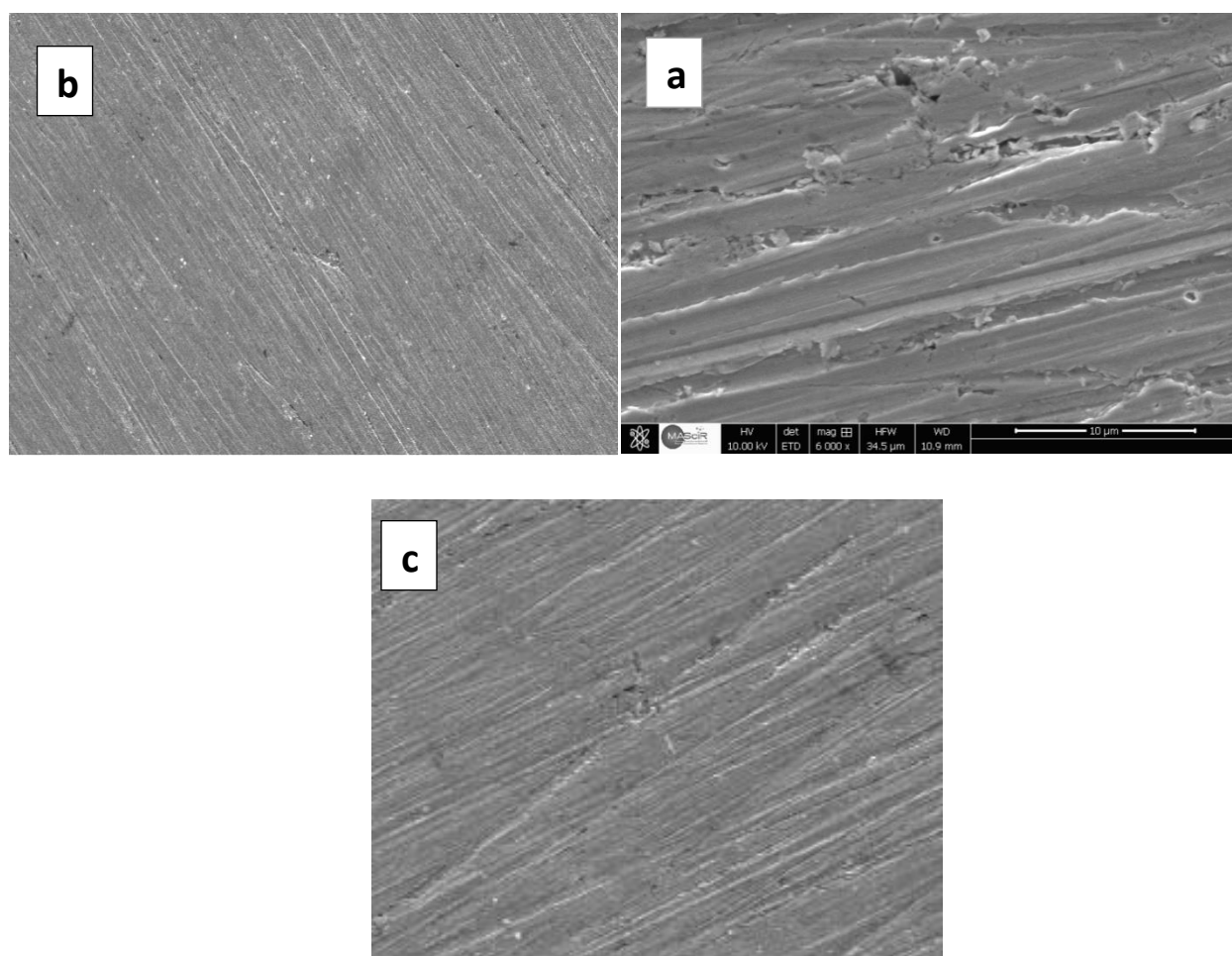


Figure 8. SEM microphotographs of copper in 0.5 M H_2SO_4 (a) without and with (b) TTB and (c) TB2HMHA after 6 h of immersion.

The surface of the corroded copper samples was found to be irregular and rough. Moreover, it was noticeable also that these microphotographs showed a heterogeneous layer exhibited a non-uniform film of the scale product formation. However, the surface morphology of copper after the addition of TTB and TB2HMHA (Figure 8b and c) displays a great surface free of corrosion products, i.e., the absence of pitting or cracks excluding the polishing lines, and the surface was smooth. It is obvious that these organic compounds are adsorbed on the surface of copper, forming a protective film by Calixarenes on the copper surface in sulfuric acid solutions [82].

3.6. Contact angle measurements.

Figure 9 shows the surface contact angles for the m-steel electrode in 0.5 M H_2SO_4 solution without and with the addition of 10^{-3}M of inhibitors TTB and TB2HMHA after exposing the m-steel to the test solutions for 6 h at room temperature.

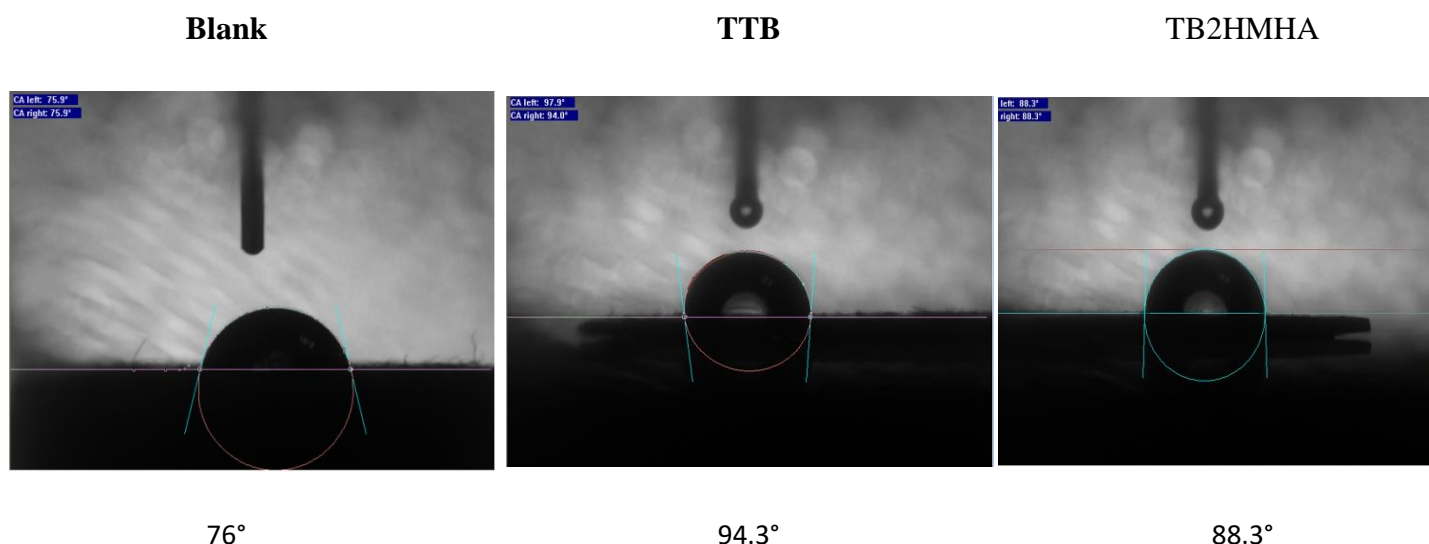


Figure 9. Contact angle measurements for metal immersed in 0.5 M H₂SO₄(Blank) and metal immersed in 0.5 M H₂SO₄containing 10⁻³M of TTB and TB2HMHA after 6 h immersion.

According to the literature, surfaces with θ below 90° are hydrophilic, whereas surfaces with θ above 90° are hydrophobic. The contact angle was determined as 76.0° in the studied corrosive media. The addition of 10⁻³M of TTB and TB2HMHA increases the contact angle from 76° to 94.3° and 88.3° for TTB and TB2HMHA, respectively. This increase is due to the adsorption of the studied products and, thus, the creation of a barrier film over the them-steel surface. Therefore, it may be claimed that the adsorption of organic species onto the steel surface improves the surface's hydrophobic nature.

4. Application

Organic corrosion inhibitors have received much attention because they provide a straightforward method for shielding metals against corrosion in an aqueous environment. As a result, there are several industrial uses for marketed corrosion inhibitors, including cooling systems, pipelines, oil and gas production facilities, boilers, and pickling procedures. Cooling water systems need the most inhibitor, and this is because inorganic inhibitors such as phosphates, tungstate, calixarenes, and molybdate are still often utilized in this industry. For these engineering aims, it is expected that the necessary inhibitor would either directly adsorb on the metal surface or form an insoluble complex with metal ions already present at the interface, resulting in the assembly of the chemisorbed film (ideal monolayer). There have been several chemical compositions for steel and its alloys that are based on organic inhibitors. Although steel has been the most extensively utilized material, additional advancement in using organic inhibitors to preserve steel from corrosion is required. However, there is growing worried about utilizing "green" chemicals for these uses, which is another reason why studies on organic corrosion inhibitors are being pushed forward. To create a chemical that can do several tasks, molecular design and the synthesis of new organic inhibitors have been identified as viable approaches. These should be carefully considered for the application's effectiveness in order to prevent using too many chemicals or providing inadequate protection. Potential interaction between the crucial

factors should also be taken into consideration for the application's convenience. Because of this, statistical analyses using information gathered from multiple pathways used to calculate the corrosion rate must be conducted. Tafel and Stern-Geary methods are generally used in the preferred approach, which is dependent on electrochemical techniques. Additionally, popular methods for assessing corrosion rate include solution test analysis and loss weight measures. With reference to current research published in pertinent disciplines, this essay focuses on the interpretations of the concerns raised.

5. Conclusions

Concluding the experimental part, it was demonstrated that all techniques used could characterize and follow the corrosion inhibition process promoted by two calixarenes compounds: TTB and TB2HMHA exhibited excellent inhibition properties for copper corrosion in 0.5 M H₂SO₄ solution, and their inhibitory efficiency increases with increasing concentration.

The obtained results showed that TTB and TB2HMHA acted as cathodic-type inhibitors of copper corrosion in 0.5 M H₂SO₄. The EIS outcomes reveal that the polarization resistance (R_p) increased as the concentrations of TTB and TB2HMHA increased. In addition, both additives have shown very good inhibitory efficacy in the corrosive medium. The adsorption characteristics of TTB and TB2HMHA were monitored following the Langmuir isotherm model. Based on the evolution of inhibition effectiveness, it can be confirmed that the adsorption of both calixarenes compounds is made by intermediate adsorption between physisorption and chemisorptions. Surface morphology studies confirmed the mitigation of copper corrosion by forming a protective film on the surface of the copper. Additionally, E_a values of the solution containing TTB and TB2HMHA are higher than that in the case of the blank medium, confirming the formation of a barrier layer on the copper surface.

Finally, the SEM images confirmed all the previous results and showed that adding calyx could inhibit copper corrosion in 0.5 M H₂SO₄. The collected findings demonstrate that the investigated compounds could be used as corrosion inhibitors for protection against the corrosion of copper in other aggressive environments.

Funding

This research received no external funding.

Acknowledgments

This research has no acknowledgment.

Conflicts of Interest

The authors declare no conflict of interest.

References

1. Esraa, E.E.; Amr M. A.; Dalia M. A.; El Gammal, O.A. Synthesis and Physicochemical Studies of Polyvinyl Alcohol Polymer Modified with Copper Thiosemicarbazide Complex. *Letters in Applied NanoBioScience*, **2021**, *10*, 2624–2636, <https://doi.org/10.33263/LIANBS104.26242636>.
2. Hanaa, M. E.; Omnia A. M.; Fouda, A. E. S. Artichoke Extract as an Eco-Friendly Corrosion Inhibitor for Zinc in 1 M Hydrochloric Acid Solution. *Letters in Applied NanoBioScience*, **2021**, *10*, 2655–2679, <https://doi.org/10.33263/LIANBS104.26552679>.
3. Qafsaoui, W.; Blanc, C.; Pebere, N.; Takenouti, H.; Shiri, A.; Mankowski, G. Quantitative characterization of protective films grown on copper in the presence of different triazole derivative inhibitors. *Electrochim. Acta*, **2002**, *47*, 4339, [https://doi.org/10.1016/S0013-4686\(02\)00486-3](https://doi.org/10.1016/S0013-4686(02)00486-3).
4. Zhang, D.Q.; Gao, L.X.; Zhou, G.D. Synergistic effect of 2-mercapto benzimidazole and KI on copper corrosion inhibition in aerated sulfuric acid solution. *Appl. Electrochem*, **2003**, *33*, 361, <https://doi.org/10.1023/A:1024403314993>.
5. Galai, M.; Ouassir, J.; Touhami, M.; Nassali, H.; Benqlilou, H.; Belhaj, T.; Berrami, K.; Mansouri, I.; Oauki, B. α -Brass and ($\alpha + \beta$) Brass Degradation Processes in Azrou Soil Medium Used in Plumbing Devices. *Journal of Bio-and Tribo-Corrosion*, **2017**, *3*, 30, <https://doi.org/10.1007/s40735-017-0087-y>.
6. Zhang, D.Q.; Gao, L.X.; Zhou, G.D. Inhibition of copper corrosion by bis-(1-benzotriazolymethylene)-(2, 5-thiadiazoly)-disulfide in chloride media. *Appl. Surf. Sci*, **2004**, *225*, 225287, <https://doi.org/10.1016/j.apsusc.2003.10.016>.
7. M'hanni, N.; Galai, M.; Anik, T.; EbnTouhami, M.; Rifi, E.H.; Asfari, Z.; Tour, R. Influence of additives selected calix [4] arenes on electroless copper plating using hypophosphite as reducing agent. *Surface Coatings Technol*, **2017**, *8*, 310, <https://doi.org/10.1016/j.surfcoat.2016.12.042>.
8. Sherif, E.M.; Park, S. Inhibition of copper corrosion in acidic pickling solutions by N-phenyl-1, 4-phenylenediamine. *Electrochim. Acta*, **2006**, *51*, 4665, <https://doi.org/10.1016/j.electacta.2006.01.007>.
9. Matos, J.B.; Pereira, L.P.; Agostinho, S.M.L.; Barcia, O.E.; Cordeiro, G.G.O.; Elia, E.D. Effect of cysteine on the anodic dissolution of copper in sulfuric acid medium. *Electroanal. Chem*, **2004**, *570*, 91-94, <https://doi.org/10.1016/j.jelechem.2004.03.020>.
10. TrabANELLI, G.; Frignani, A.; Monticelli, C.; Zucchi, F. Alkyl-benzotriazole derivatives as inhibitors of iron and copper corrosion. *Int. J. Corros. Scale Inhib*, **2015**, *4*, 96–10, <https://doi.org/10.17675/2305-6894-2015-4-1-096-107>.
11. Rbaa M.; Ouakki M.; Galai M.; Berishad A.; Lakhrissi B.; Jama C.; Warad I.; Zarrouk A.; Simple preparation and characterization of novel 8-Hydroxyquinoline derivatives as effective acid corrosion inhibitor for mild steel: Experimental and theoretical studies, *Colloids and Surfaces A: Physicochemical and Engineering Aspects* **2020**, *602*, 125094, <https://doi.org/10.1016/j.colsurfa.2020.125094>.
12. Dahmani, K.; Galai, M.; Ouakki, M.; Cherkaoui, M.; Tour, R.; Erkan, S.; Kaya, S.; El Ibrahim, B. Quantum chemical and molecular dynamic simulation studies for the identification of the extracted cinnamon essential oil constituent responsible for copper corrosion inhibition in acidified 3.0 wt% NaCl medium, *Inorganic Chemistry Communications* **2021**, *124*, 108409, <https://doi.org/10.1016/j.inoche.2020.108409>.
13. Kozaderov, O.A.; Shikhaliev, Kh.S.; Prabhakar, Ch.; Shevtsov, D.S.; Kruzilin, A.A.; Komarova, E.S.; Potapov, A. Yu.; Zartsyn, I.D. Copper corrosion inhibition in chloride environments by 3-(N-hetaryl)-5-amino-1H-1,2,4-triazoles. *Int. J. Corros. Scale Inhib*, **2019**, *8*, 422–436, <https://doi.org/10.17675/2305-6894-2019-8-2-19>.
14. Khrifou, R.; Galai, M.; El Bakri, H.; Larhzil, H.; Tour, R.; EbnTouhami, M.; Ramli, Y. Corrosion inhibition of brass in phosphoric acid solution by 2-(5-methyl-2-nitro-1H-imidazol-1-yl) ethyl benzoate, *Chemical Data Collections* **2019**, *24*, 100303, <https://doi.org/10.1016/j.cdc.2019.100303>.
15. Hsissou, Rachid, *et al.* "Theoretical and electrochemical studies of the coating behavior of a new epoxy polymer: hexaglycidyl ethylene of methylene dianiline (HGEMDA) on E24 steel in 3.5% NaCl, *Port Electrochim Acta*, **2018**, *36*, 101-117, <https://doi.org/10.4152/pea.201802101>.
16. Rbaa, M.; Fardioui, M.; Chandrabhan, V.; Abousalem, Ashraf, S.; Galai, M.; Ebenso, E.E.; Guedira, T.; Lakhrissi, B.; Warad, I.; Zarrouk, A. 8-Hydroxyquinoline based chitosan derived carbohydrate polymer as biodegradable

- and sustainable acid corrosion inhibitor for mild steel: Experimental and computational analyses. *International Journal of Biological Macromolecules*, **2020**, *155*, 645-655, <https://doi.org/10.1016/j.ijbiomac.2020.03.200>.
17. Ouakki, M.; Galai, M.; Aribou, Z.; Benzekri, Z.; El Assiri, E.H.; Dahmani, K.; Ech-chihbi, E.; Abousalem, A.S.; Boukhris, S.; Cherkaoui, M. Detailed experimental and computational explorations of pyran derivatives as corrosion inhibitors for mild steel in 1.0 M HCl: Electrochemical/surface studies, DFT modeling, and MC simulation. *Journal of Molecular Structure*, **2022**, *1261*, 132784, <https://doi.org/10.1016/j.molstruc.2022.132784>.
 18. Hsissou, Rachid, *et al.* New epoxy composite polymers as a potential anticorrosive coatings for carbon steel in 3.5% NaCl solution: Experimental and computational approaches. *Chemical Data Collections*, **2021**, *31* 100619, <https://doi.org/10.1016/j.cdc.2020.100619>.
 19. Hsissou, Rachid, *et al.* Performance of curing epoxy resin as potential anticorrosive coating for carbon steel in 3.5% NaCl medium: Combining experimental and computational approaches. *Chemical Physics Letters*, **2021**, *783*, 139081, <https://doi.org/10.1016/j.cplett.2021.139081>.
 20. Galai, M.; Rbaa, M.; Ouakki, M.; Dahmani, K.; Kaya, S.; Arrousse N.; Dkhireche, N.; Briche, S.; Lakhrissi, B.; EbnTouhami, M. Functionalization effect on the corrosion inhibition of novel eco-friendly compounds based on 8-hydroxyquinoline derivatives: Experimental, theoretical and surface treatment. *Chemical Physics Letters*, **2021**, *77*, 138700, <https://doi.org/10.1016/j.cplett.2021.138700>.
 21. Hsissou, R., *et al.* Insight into the corrosion inhibition of novel macromolecular epoxy resin as highly efficient inhibitor for carbon steel in acidic mediums: Synthesis, characterization, electrochemical techniques, AFM/UV–Visible and computational investigations, *Journal of Molecular Liquids*, **2021**, *337*, 116492, <https://doi.org/10.1016/j.molliq.2021.116492>.
 22. Hsissou, Rachid. Review on epoxy polymers and its composites as a potential anticorrosive coatings for carbon steel in 3.5% NaCl solution: Computational approaches. *Journal of Molecular Liquids*, **2021**, *336*, 116307, <https://doi.org/10.1016/j.molliq.2021.116307>.
 23. Galai, M.; Rbaa, M.; Ouakki, M.; Guo, L.; Dahmani, Nouneh, K.; Briche, S.; Lakhrissi, B.; Dkhireche, N.; Ebn Touhami, M. Effect of alkyl group position on adsorption behavior and corrosion inhibition of new naphthol based on 8-hydroxyquinoline: Electrochemical, surface, quantum calculations and dynamic simulations. *Journal of Molecular Liquids* **2021**, *335*, 116552, <https://doi.org/10.1016/j.molliq.2021.116552>.
 24. Hsissou, Rachid, *et al.* Synthesis and anticorrosive properties of epoxy polymer for CS in [1 M] HCl solution: Electrochemical, AFM, DFT and MD simulations. *Construction and Building Materials*, **2021**, *270*, 121454, <https://doi.org/10.1016/j.conbuildmat.2020.121454>.
 25. Kılınççeker, G.; Baş, M.; Zarifi, F.; Sayın, K. Experimental and Computational Investigation for (E)-2-hydroxy-5-(2-benzylidene) Aminobenzoic Acid Schiff Base as a Corrosion Inhibitor for Copper in Acidic Media. *Iran J Sci. Technol. Trans. Sci.* **2020**, *45*, 515-527, <https://doi.org/10.1007/s40995-020-01015-x>.
 26. Ouakki, M.; Galai, M.; Benzekri, Z.; Chandrabhan Verma, Ech-chihbi, E.; Kaya, S.; Boukhris, S.; Ebenso, Eno E.; Ebn Touhami, M.; Cherkaoui, M. Insights into corrosion inhibition mechanism of mild steel in 1 M HCl solution by quinoxaline derivatives: electrochemical, SEM/EDAX, UV-visible, FT-IR and theoretical approaches, *Colloids Surf, A Physicochem Eng Asp*, **2021**, *611*, 125810, <https://doi.org/10.1016/j.colsurfa.2020.125810>.
 27. Aadad, H.E.; Galai, M.; Ouakki, M.; Elgendy, A.; Touhami, M.E.; Chahine, A. Improvement of the corrosion resistance of mild steel in sulfuric acid by new organic-inorganic hybrids of Benzimidazole-Pyrophosphate: Facile synthesis, characterization, experimental and theoretical calculations (DFT and MC). *Surfaces and Interfaces* **2021**, *24*, 101084, <https://doi.org/10.1016/j.surfin.2021.101084>.
 28. Guo, L.; Obot, I.B.; Zheng, X.; Shen, X.; Qiang, Y.; Kaya, S.; Kaya, C. Theoretical insight into an empirical rule about organic corrosion inhibitors containing nitrogen, oxygen, and sulfur atoms. *Applied Surface Science* **2017**, *406*, 301-306, <https://doi.org/10.1016/j.apsusc.2017.02.134>.
 29. Ouass, A.; Galai, M.; Ouakki, M.; Ech-Chihbi, E.; Kadiri, L.; Hsissou, R.; Essaadaoui, Y.; Berisha, A.; Cherkaoui, M.; Lebkiri, A.; Rifi, E. H. Poly (sodium acrylate) and Poly (acrylic acid sodium) as an eco-friendly corrosion inhibitor of mild steel in normal hydrochloric acid: experimental, spectroscopic and theoretical approach. *Journal of Applied Electrochemistry* **2021**, *51*, 1009-1032, <https://doi.org/10.1007/s10800-021-01556-y>.

30. Feng, L.; Zhang, S.; Feng, Y.; Ren, X.; Lu, H.; Tan, B.; Chen, S. Self-aggregate nanoscale copolymer of new synthesized compounds efficiently protecting copper corrosion in sulfuric acid solution. *Chemical Engineering Journal* **2020**, *394*, 124909, <https://doi.org/10.1016/j.cej.2020.124909>.
31. Abouchane, M.; Dkhireche, N.; Rbaa, M.; Benhiba, F.; Ouakki, M.; Galai, M.; Lakhrissi, B.; Zarrouk, A.; Ebn Touhami, M. Insight into the corrosion inhibition performance of two quinoline-3-carboxylate derivatives as highly efficient inhibitors for mild steel in acidic medium: Experimental and theoretical evaluations. *Journal of Molecular Liquids*, **2022**, *360*, 119470, <https://doi.org/10.1016/j.molliq.2022.119470>.
32. Zhang, W.; Ma, R.; Liu, H.; Liu, Y.; Li, S.; Niu, L. Electrochemical and surface analysis studies of 2-(quinolin-2-yl)quinazolin-4(3H)-one as corrosion inhibitor for Q235 steel in hydrochloric acid. *Journal of Molecular Liquids* **2016**, *222*, 671-679, <https://doi.org/10.1016/j.molliq.2016.07.119>.
33. El aadad, H.; Galai, M.; Chahine, A.; Ebn Touhami, M. Synthesis, characterization and thermal properties of 2,2'-dibenzimidazolyl butane as a novel corrosion inhibitors for mild steel in sulfuric acid. *Surf. Rev. Lett* **2020**, *27*, 1950115, <https://doi.org/10.1142/S0218625X19501154>.
34. Kuznetsov, Yu.I.; Kuznetsov, I.A.; Andreeva, N.P. Adsorption of sodium tridecanoate on copper from aqueous solutions and copper protection from atmospheric corrosion. *Int. J. Corros. Scale Inhib*, **2018**, *7*, 648-656, <https://doi.org/10.17675/2305-6894-2018-7-4-11>.
35. Gutsche, C.D.; Dhawan, B.; No, K.H.; Muthukrishnan, R. Calixarenes. 4. The synthesis, characterization, and properties of the calixarenes from p-tert-butylphenol. *Journal of the American Chemical Society*, **1981**, *103*, 3782-3792, <https://doi.org/10.1021/ja00403a028>.
36. Şahin, M.; Gece, G.; Karci, F.; Bilgiç, S. Experimental and theoretical study of the effect of some heterocyclic compounds on the corrosion of low carbon steel in 3.5% NaCl medium. *Journal of Applied Electrochemistry* **2008**, *38*, 809-815, <https://doi.org/10.1007/s10800-008-9517-3>.
37. Ouakki, M.; Rbaa, M.; Galai, M.; Lakhrissi, B.; Rifi, E.H.; Cherkaoui, M. Experimental and Quantum Chemical Investigation of Imidazole Derivatives as Corrosion Inhibitors on Mild Steel in 1.0 M Hydrochloric Acid, *Journal of Bio-and Tribo-Corrosion* **2018**, *4*, 35, <https://doi.org/10.1007/s40735-018-0151-2>.
38. da Silva, A.B.; D'Elia, E.; da Cunha Ponciano Gomes, J.A. Carbon steel corrosion inhibition in hydrochloric acid solution using a reduced Schiff base of ethylenediamine. *Corrosion Science* **2010**, *52*, 788-793, <https://doi.org/10.1016/j.corsci.2009.10.038>.
39. Naderi, E.; Jafari, A.H.; Ehteshamzadeh, M.; Hosseini, M.G. Effect of carbon steel microstructures and molecular structure of two new Schiff base compounds on inhibition performance in 1M HCl solution by EIS. *Materials Chemistry and Physics* **2009**, *115*, 852-858, <https://doi.org/10.1016/j.matchemphys.2009.03.002>.
40. Ben Hmamou, D.; Salghi, R.; Zarrouk, A.; Zarrok, H.; Benali, O.; Errami, M.; Hammouti, B. Inhibition effect of horehound (*Marrubium vulgare* L.) extract towards C38 steel corrosion in HCl solution. *Research on Chemical Intermediates* **2013**, *39*, 3291-3302, <https://doi.org/10.1007/s11164-012-0840-2>.
41. Bentiss, F.; Lagrenée, M.; Traisnel, M.; Hornez, J. C. The corrosion inhibition of mild steel in acidic media by a new triazole derivative. *Corrosion Science* **1999**, *41*, 789-803, [https://doi.org/10.1016/S0010-938X\(98\)00153-X](https://doi.org/10.1016/S0010-938X(98)00153-X).
42. Ech-chihbi, E.; Belghiti, M.E.; Salim, R.; Oudda, H.; Taleb, M.; Benchat, N.; Hammouti, B.; El-Hajjaji, F. Experimental and computational studies on the inhibition performance of the organic compound "2-phenylimidazo [1, 2-a] pyrimidine-3-carbaldehyde" against the corrosion of carbon steel in 1.0 M HCl solution, *Journal Surfaces and Interfaces* **2017**, *9*, 206-217, <https://doi.org/10.1016/j.surfin.2017.09.012>.
43. Tao, Z.; Zhang, S.; Li, W.; Hou, B. Corrosion inhibition of mild steel in acidic solution by some oxo-triazole derivatives. *Corrosion Science* **2009**, *51*, 2588-2595, <https://doi.org/10.1016/j.corsci.2009.06.042>.
44. Ferreira, E.S.; Giacomelli, C.; Giacomelli, F.C.; Spinelli, A. Evaluation of the inhibitor effect of l-ascorbic acid on the corrosion of mild steel. *Materials Chemistry and Physics* **2004**, *83*, 129-134, <https://doi.org/10.1016/j.matchemphys.2003.09.020>.
45. Roy, P.; Karfa, P.; Adhikari, U.; Sukul, D. Corrosion inhibition of mild steel in acidic medium by polyacrylamide grafted Guar gum with various grafting percentage: Effect of intramolecular synergism. *Corrosion Science* **2014**, *88*, 246-253, <https://doi.org/10.1016/j.corsci.2014.07.039>.
46. Moradi, M.; Duan, J.; Du, X. Investigation of the effect of 4,5-dichloro-2-n-octyl-4-isothiazolin-3-one inhibition on the corrosion of carbon steel in *Bacillus* sp. inoculated artificial seawater. *Corrosion Science* **2013**, *69*, 338-345, <https://doi.org/10.1016/j.corsci.2012.12.017>.

47. Tang, Y.; Zhang, F.; Hu, S.; Cao, Z.; Wu, Z.; Jing, W. Novel benzimidazole derivatives as corrosion inhibitors of mild steel in the acidic media. Part I: Gravimetric, electrochemical, SEM and XPS studies. *Corrosion Science* **2013**, *74*, 271-282, <https://doi.org/10.1016/j.corsci.2013.04.053>.
48. Khaled, K.F. Electrochemical investigation and modeling of corrosion inhibition of aluminum in molar nitric acid using some sulphur-containing amines. *Corrosion Science* **2010**, *52*, 2905-2916, <https://doi.org/10.1016/j.corsci.2010.05.001>.
49. Aljourani, J.; Raeissi, K.; Golozar, M.A. Benzimidazole and its derivatives as corrosion inhibitors for mild steel in 1M HCl solution. *Corrosion Science* **2009**, *51*, 1836-1843, <https://doi.org/10.1016/j.corsci.2009.05.011>.
50. El-Haddad, M.N.; Fouda, A.-A. Evaluation of Curam drug as an ecofriendly corrosion inhibitor for protection of stainless steel-304 in hydrochloric acid solution: Chemical, electrochemical, and surface morphology studies, *J. Chin. Chem. Soc.* **2021**, *68* (5), 826-836, <https://doi.org/10.1002/jccs.202000409>.
51. Quraishi, M.A.; Rawat, J. Influence of iodide ions on inhibitive performance of tetraphenyl-dithia-octaazacyclotetradeca-hexaene (PTAT) during pickling of mild steel in hot sulfuric acid. *Materials Chemistry and Physics* **2001**, *70*, 95-99, [https://doi.org/10.1016/S0254-0584\(00\)00459-4](https://doi.org/10.1016/S0254-0584(00)00459-4).
52. Amin, M.A.; Abd El-Rehim, S.S.; El-Sherbini, E.E.F.; Bayoumi, R.S. The inhibition of low carbon steel corrosion in hydrochloric acid solutions by succinic acid: Part I. Weight loss, polarization, EIS, PZC, EDX and SEM studies. *Electrochimica Acta*, **2007**, *52*, 3588-3600, <https://doi.org/10.1016/j.electacta.2006.10.019>.
53. Rahmouni, K.; Keddami, M.; Srhiri, A.; Takenouti, H. Corrosion of copper in 3% NaCl solution polluted by sulphide ions. *Corrosion Science* **2005**, *47*, 3249-3266, <https://doi.org/10.1016/j.corsci.2005.06.017>.
54. Kardas, G. The inhibition effect of 2- thiobarbituric acid on the corrosion performance of mild steel in HCl solutions. *J. Materials Science* **2005**, *41*, 337-343, <https://doi.org/10.1007/s11003-005-0170-2>.
55. Behpour, M.; Ghoreishi, S. M.; Soltani, N.; Salavati-Niasari, M.; Hamadani, M.; Gandomi, A. Electrochemical and theoretical investigation on the corrosion inhibition of mild steel by thiosalicylaldehyde derivatives in hydrochloric acid solution. *Corros. Sci* **2008**, *50*, 2172-2181, <https://doi.org/10.1016/j.corsci.2008.06.020>.
56. Singh, A. K.; Quraishi, M. A. Effect of 2,2' benzothiazolyl disulfide on the corrosion of mild steel in acid media. *Corros. Sci* **2009**, *51*, 2752-2760, <https://doi.org/10.1016/j.corsci.2009.07.011>.
57. Aljourani, J.; Raeissi, K.; Golozar, M.A. Benzimidazole and its derivatives as corrosion inhibitors for mild steel in 1M HCl solution. *Corros. Sci* **2009**, *51*, 1836-1843, <https://doi.org/10.1016/j.corsci.2009.05.011>.
58. Hsu, C. H.; Mansfeld, F. Concerning the conversion of the constant phase element parameter Y0 into a capacitance. *Corrosion* **2001**, *57*, 747, <https://doi.org/10.5006/1.3280607>.
59. Ouakki, M.; Galai, M.; Rbaa, M.; Abousalem, A. S.; Lakhrissi, B.; Rifi, E. H.; Cherkaoui, M. Quantum chemical and experimental evaluation of the inhibitory action of two imidazole derivatives on mild steel corrosion in sulphuric acid medium. *Heliyon* **2019**, *5*, e02759, <https://doi.org/10.1016/j.heliyon.2019.e02759>.
60. Tian, H.; Li, W.; Cao, K.; Hou, B. Potent inhibition of copper corrosion in neutral chloride media by novel non-toxic thiadiazole derivatives. *Corrosion Science* **2013**, *73*, 281-291, <https://doi.org/10.1016/j.corsci.2013.04.017>.
61. Tian, H.; Hou, W.; Li, B. Novel application of a hormone biosynthetic inhibitor for the corrosion resistance enhancement of copper in synthetic seawater. *Corros. Sci* **2011**, *53*, 3435-3445, <https://doi.org/10.1016/j.corsci.2011.06.025>.
62. M'hanni, N.; Galai, M.; Anik, T.; Ebn Touhami, M.; Rifi, E.H.; Asfari, Z.; Tourir, R. Influence of additives selected calix[4]arenes on electroless copper plating using hypophosphite as reducing agent. *Surface & Coatings Technology* **2017**, *310*, 8-16, <https://doi.org/10.1016/j.surfcoat.2016.12.042>.
63. Ouakki, M.; Galai, M.; Benzekri, Z.; Verma, C.; Ech-chihbi, E.; Kaya, S.; Boukhris, S.; Ebenso, E.E.; EbnTouhami, M.; Cherkaoui, M. Insights into corrosion inhibition mechanism of mild steel in 1 M HCl solution by quinoxaline derivatives: electrochemical, SEM/EDAX, UV-visible, FT-IR and theoretical approaches. *Colloids and Surfaces A: Physicochemical and Engineering Aspects* **2021**, *611*, 125810, <https://doi.org/10.1016/j.colsurfa.2020.125810>.
64. Lopez, D.A.; Simison, S.N.; de Sanchez, S.R. The influence of steel microstructure on CO₂ corrosion. EIS studies on the inhibition efficiency of benzimidazole. *Electrochim. Acta* **2003**, *48*, 845-854, [https://doi.org/10.1016/S0013-4686\(02\)00776-4](https://doi.org/10.1016/S0013-4686(02)00776-4).
65. Li, X.; Xie, X.; Deng, S.; Du, G. Two phenylpyrimidine derivatives as new corrosion inhibitors for cold rolled steel in hydrochloric acid solution. *Corros. Sci* **2014**, *87*, 27-39, <https://doi.org/10.1016/j.corsci.2014.05.017>.

66. Rbaa, M.; Benhiba, F.; Galai, M.; S. Abousalem, A.; Ouakki, M.; Lai, Chin-Hung.; Lakhrissi, B.; Jama, C.; Warad, I.; Ebn Touhami, M.; Zarrouk, A. Synthesis and characterization of novel Cu (II) and Zn (II) complexes of 5-[(2-Hydroxyethyl) sulfanyl] methyl]-8-hydroxyquinoline as effective acid corrosion inhibitor by experimental and computational testings. *Chemical Physics Letters* **2020**, *754*, 137771, <https://doi.org/10.1016/j.cplett.2020.137771>.
67. Melian, R.; Radi, M.; Galai, M.; Ouakki, M.; Ech-chihbi, E.; Dkhirche, N.; Lei, Guo.; EbnTouhami, M. Anticorrosion properties of 5, 5'-dithiobis-(2-nitrobenzoic acid) and sodium sulfite compounds for aluminum alloy 2024-T3 in saline solution: Electrochemical, characterization and theoretical investigations. *Journal of Molecular Liquids* **2021**, *331*, 115661, <https://doi.org/10.1016/j.molliq.2021.115661>.
68. Hosseini, M.; Mertens, S.F.L.; Ghorbani, M.; Arshadi, M.R. Asymmetrical Schiff bases as inhibitors of mild steel corrosion in sulphuric acid media. *Mater Chem Phys*, **2003**, *78*, 800–808, [https://doi.org/10.1016/S0254-0584\(02\)00390-5](https://doi.org/10.1016/S0254-0584(02)00390-5).
69. Roy, P.; Karfa, P.; Adhikari, U.; Sukul, D. Corrosion inhibition of mild steel in acidic medium by polyacrylamide grafted Guar gum with various grafting percentage: Effect of intramolecular synergism. *Corros. Sci* **2014**, *88*, 246–253, <https://doi.org/10.1016/j.corsci.2014.07.039>.
70. Ech-chihbi, E.; Nahlé, A.; Salim, R.; Oudda, H.; El Hajjaji, F.; El Kalai, F.; El Aatiaoui, A.; Taleb, M. An Investigation into Quantum Chemistry and Experimental Evaluation of Imidazopyridine Derivatives as Corrosion Inhibitors for C-Steel in Acidic Media. *J Bio TriboCorros* **2019**, *5*, 24, <https://doi.org/10.1007/s40735-019-0217-9>.
71. Flis, J.; Zakroczyński, T. Impedance study of reinforcing steel in simulated pore solution with tannin. *J. Electrochem. Soc* **1996**, *143*, 2458, <https://iopscience.iop.org/article/10.1149/1.1837031>.
72. Bentiss, F.; Lebrini, M.; Lagrenée, M. Thermodynamic characterization of metal dissolution and inhibitor adsorption processes in mild steel/2, 5-bis (n-thienyl)-1, 3, 4-thiadiazoles/hydrochloric acid system. *Corros. Sci* **2005**, *47*, 2915–2931, <https://doi.org/10.1016/j.corsci.2005.05.034>.
73. Khamis, E.; Bellucci, F.; Latanision, R. M.; El-Ashry, E. S. H. Acid corrosion inhibition of nickel by 2-(Triphenylphosphorylidene) succinic anhydride. *Corrosion* **1991**, *47*, 677–686, <https://doi.org/10.5006/1.3585307>.
74. Yadav, M.; Gope, L.; Kumari, N.; Yadav, P. Corrosion inhibition performance of pyranopyrazole derivatives for mild steel in HCl solution: Gravimetric, electrochemical and DFT studies. *J. Mol. Liq* **2016**, *216*, 78–86, <https://doi.org/10.1016/j.molliq.2015.12.106>.
75. Ituen, E. B.; Solomon, M. M.; Umoren, S. A.; Akaranta, O. Corrosion inhibition by amitriptyline and amitriptyline based formulations for steels in simulated pickling and acidizing media, *J Pet Sci Eng* **2019**, *174*, 984–996, <https://doi.org/10.1016/j.petrol.2018.12.011>.
76. Ouakki, M.; Galai, M.; Rbaa, M.; Abousalem, Ashraf S.; Lakhrissi, B.; Rifi, E. H.; Cherkaoui, M. Investigation of imidazole derivatives as corrosion inhibitors for mild steel in sulfuric acidic environment: experimental and theoretical studies. *Ionics*. **2020**, *26*, 5251–5272, <https://doi.org/10.1007/s11581-020-03643-0>.
77. Murulana, L.C.; Kabanda, M.M.; Ebenso, E.E. Investigation of the adsorption characteristics of some selected sulphonium derivatives as corrosion inhibitors at mild steel/hydrochloric acid interface: Experimental, quantum chemical and QSAR studies. *Journal of Molecular Liquids*, **2016**, *215*, 763–779, <https://doi.org/10.1016/j.molliq.2015.12.095>.
78. Fergachi, O.; Benhiba, F.; Rbaa, M.; Ouakki, M.; Galai, M.; Touir, R.; Lakhrissi, B.; Oudda, H.; Ebn Touhami, M. Corrosion inhibition of ordinary steel in 5.0 M HCl medium by benzimidazole derivatives: electrochemical, UV–visible spectrometry, and DFT calculations. *Journal of Bio-and Tribo-Corrosion*, **2019**, *5*, 21, <https://doi.org/10.1007/s40735-018-0215-3>.
79. Geethanjali, R.; Subhashini, S. Thermodynamic Characterization of Metal Dissolution and Adsorption of Polyvinyl Alcohol-Grafted Poly(Acrylamide Vinyl Sulfonate) on Mild Steel in Hydrochloric Acid. *Portugaliae Electrochim. Acta* **2015**, *33*, 35–48, <https://doi.org/10.4152/pea.201501035>.
80. Yadav, M.; Kumar, S.; Tiwari, N.; Bahadur, I.; Ebenso, E. E. Experimental and quantum chemical studies of synthesized triazine derivatives as an efficient corrosion inhibitor for N80 steel in acidic medium. *J Mol Liq* **2015**, *212*, 151–67, <https://doi.org/10.1016/j.molliq.2015.09.019>.

81. Martinez, S.; Stern, I. Thermodynamic characterization of metal dissolution and inhibitor adsorption processes in the low carbon steel/mimosa tannin/sulfuric acid system. *Appl. Surf. Sci* **2002**, *199*, 83-89, [https://doi.org/10.1016/S0169-4332\(02\)00546-9](https://doi.org/10.1016/S0169-4332(02)00546-9).
82. Prabhu, R. A.; Venkatesha, T. V.; Shanbhag, A. V.; Kulkarni, G. M.; Kalkhambkar, R.G. Inhibition effects of some Schiff's bases on the corrosion of mild steel in hydrochloric acid solution. *Corros. Sci* **2008**, *50*, 3356-3362, <https://doi.org/10.1016/j.corsci.2008.09.009>.